THE JOURNAL OF PHYSICAL CHEMISTRY B

Article

pubs.acs.org/JPCB

Controlling the Morphology of Poly(*N*-cyanoethylpyrrole)

Georgina Fabregat,[†,‡] Carlos Alemán,*[,†,‡] Maria T. Casas,[†] and Elaine Armelin*[,†,‡]

[†]Departament d'Enginyeria Química, ETSEIB, Universitat Politècnica de Catalunya, Av. Diagonal 647, 08028, Barcelona, Spain

[‡]Center for Research in Nano-Engineering, Universitat Politècnica de Catalunya, Campus Sud, Edifici C', C/Pasqual i Vila s/n, Barcelona E-08028, Spain

Supporting Information

ABSTRACT: The morphology of poly(*N*-cyanoethylpyrrole) has been controlled through the polymerization process. This polymer has been prepared by anodic polymerization, chemical oxidative polymerization in emulsion medium, and layer-by-layer templating polymerization. Anodic polymerization using $LiClO_4$ as supporting electrolyte provides compact films, in which the oxidation degree is controlled through the thickness, useful for the microdetection of dopamine. Chemical polymerization using $FeCl_3$ as oxidant agent results in very well-defined microspheres with porous internal structure, which may be useful in molecular loading and transport processes. Finally, the layer-by-layer templating technique produces core−shell particles of controlled size and thickness. Moreover, these core−shell particles can be easily converted in hollow microspheres by removing the template.

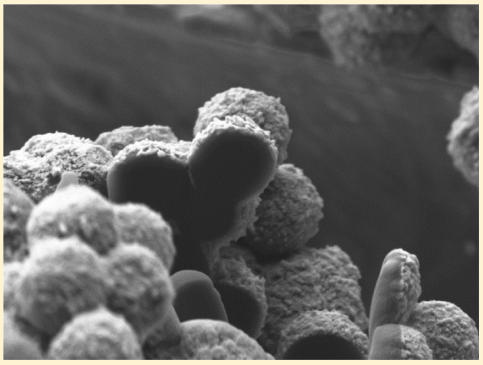

INTRODUCTION

Many of the nanostructured materials currently under development draw their inspiration from the structures found in nature.[1−3] Highly sophisticated morphologies and functions have been achieved using supramolecular architectures of polymer structures.[4] Within this context, micro- and nanostructures based on conducting polymers (CPs) is a field of current interest. CPs are a class of important materials with many potential applications because of their low density, large specific area, high stability and surface permeability, and good electrochemical properties.

In general, the structure of CPs is moderately affected by the experimental conditions used in the polymerization process. For example, the roughness, regularity, and porosity of the spongy morphology of electrochemically produced poly(3,4-ethylenedioxythiophene), an extensively studied CP with very important technological applications,[5,6] are known to depend on factors such as the applied potential, polymerization time (i.e., the thickness of the sample), the solvent, the supporting electrolyte that acts as doping agent, and the substrate used for polymer deposition.[7−13] Much higher variability can be obtained using an alternative synthetic process based on templates. These approaches are typically described as the one-step electrochemical generation of CP in a solid substrate assisted by a solid or soft template mechanism. Thus, the generation of CP micro- and nanostructures can be carried out using solid templates with well-defined shapes (e.g., porous alumina membranes or polystyrene colloidal nanoparticles) limiting the size of the materials,[14,15] or "soft" templates formed by assemblies of molecules (e.g., surfactants and gases).[16,17] This approach has been used to prepare microspheres, microcrocks, microbowls, microbarrels, micropunpkins, microbottles, and microdoughnuts of polypyrrole and poly(*N*-methylpyrrole), abbreviated PPy and PNMPy, respectively.[18−23]

In this work, we show how to exert a drastic control on the structure and morphology of poly(*N*-cyanoethylpyrrole), hereafter abbreviated PNCPy (Scheme 1), through the polymerization method. More specifically, we report the very different morphologies and microstructures found for this material when it is prepared by anodic polymerization, oxidative polymerization in emulsion medium, and layer-by-layer (LbL) templating technique. PNCPy was found to be highly sensitive to dopamine, presenting a very fast and effective response even when the concentration of such neurotransmitter is of 100 μM only (i.e., the concentration of dopamine in the synaptic region is 1.6 mM).[24] However, despite such promising biomedical application, the number of studies devoted to examine the structure of this CP is very scarce. Thus, although PNCPy has been obtained and characterized using anodic polymerization

Scheme 1

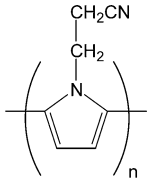

PNCPy

Received: January 26, 2012
Revised: March 16, 2012
Published: April 13, 2012

methods,[25−27] the structures of the materials prepared by the LbL procedure and oxidative polymerization have not been reported yet.

METHODS

Materials. *N*-(2-Cyanoethyl)pyrrole (NCPy), acetonitrile, and anhydrous lithium perchlorate ($LiClO_4$) of analytical reagent grade were purchased from Sigma-Aldrich (Spain). The monomer was used freshly distilled.

Electrochemical Synthesis of Poly[*N*-(2-cyanoethyl)-pyrrole] (PNCPy) Films. PNCPy films were prepared by chronoamperometry (CA) under a constant potential of 1.40 V. Electrochemical experiments were performed on an Autolab PGSTAT302N equipped with the ECD module (Ecochimie, The Netherlands), which allows one to measure very low current densities (100 μA to 100 pA), using a three-electrode two-compartment cell under nitrogen atmosphere (99.995% in purity) at room temperature. The reference electrode was a saturated Ag|AgCl electrode, whereas platinum sheets of 0.50 × 0.70 cm^2 were used as counter electrode. A glassy carbon electrode (GCE) was used as the working electrode (4.11 mm^2), its surface being polished with alumina powder and cleaned by ultrasonication before each trial. PNCPy was electrochemically deposited on the GCE using 70 mL of the corresponding monomer solution (10 mM) in acetonitrile containing 0.1 M $LiClO_4$ as supporting electrolyte. The polymerization time (θ) varied from 20 to 300 s.

Oxidative Polymerization in Emulsion Medium. A solution of NCPy (0.63 mmol) in 4.2 mL of ethanol was added to deionized water (7.0 mL) under magnetic stirring. After the monomer was completely dispersed (15 min), an excess of oxidant agent, 0.696 g of $FeCl_3{\cdot}6H_2O$ (2.5 mmol in 2.8 mL of deionized water), was added slowly into the vessel at 25 °C. After oxidant addition, the temperature was increased to 70 °C, and the reactants were stirred for 24 h. The resulting product was washed repeatedly with deionized water and ethanol. Finally, PNCPy, which was obtained as a dark-brown powder, was dried under vacuum oven at 40 °C for 48 h.

Layer-by-Layer Assembly Polymerization. *Preparation of Polystyrene Microspheres.* Polystyrene (PS) microspheres were prepared following the procedure described by Lascelles et al.[28] In a three-necked round flask provided with magnetic stirring and a condenser, poly(*N*-vinylpyrrolidone) (PVP) stabilizer (3.8 g) dissolved in isopropyl alcohol (180 mL) was heated until 70 °C for 1 h under nitrogen atmosphere. After this, a solution of α-azoisobutyronitrile (AIBN, 0.25 g) and styrene monomer (25 g) was added dropwise to the reaction vessel. The mixture, which was vigorously stirred at 70 °C for 24 h, was left for cooling at room temperature. The resulting emulsion was centrifuged several times and washed repeatedly with deionized water to remove the PVP stabilizer excess. The chemical composition of the PS samples was evaluated with FTIR spectroscopy, while the size of the latex particles was determined by scanning electron microscopy (SEM) and transmission electron microscopy (TEM).

Preparation of Polystyrene Sulfonated Microspheres. PS microparticles (10% in deionized water, 3 mL) and concentrated sulfuric acid (98%, 11 mL) were introduced into a 30 mL centrifuge tube. The sulfonation reaction was allowed to take place at 40 °C under magnetic stirring for 24 h and reflux. After this, the vessel was cooled to room temperature. The product was separated by repeated centrifugation (6000 rpm) and washed with an excess of ethanol. Finally, a white fine powder made of sulfonated PS (PSS) core−shell particles was obtained after drying under vacuum for 48 h.

Preparation of PNCPy/PSS. PSS powder (0.06 g) was dispersed in 3.5 mL of deionized water. Next, a solution of NCPy (0.17 mmol) in 4.2 mL of ethanol was added to the PSS suspension under magnetic stirring. The monomer/PSS mixture was stirred during 15 min, and then 0.19 g of $FeCl_3{\cdot}6H_2O$ (0.7 mmol in 2 mL of deionized water) was subsequently added. The polymerization process took place at 70 °C during 24 h. The resulting PNCPy/PSS particles were purified after several centrifugations washing with deionized water and ethanol. Finally, the material was dried under vacuum for 48 h. This polymerization process was repeated two times to achieve a suitable PNCPy thickness.

Preparation of PNCPy Hollow Microspheres. The PSS core was removed from PNCPy/PSS core−shell particles by dispersing the latter into tetrahydrofuran (THF, 11 mL) under magnetic stirring for 48 h at room temperature. The resulting product was washed by repeated centrifugation with ethanol and afterward was dried in a vacuum at 40 °C for 48 h.

Analytical Techniques. *Scanning Electron Microscopy (SEM).* SEM studies were carried out using a Focused Ion Bean Zeiss Neon40 scanning electron microscope equipped with an energy dispersive X-ray spectroscopy (EDS) system and operating at 5 kV. Samples were mounted on a double-sided adhesive carbon disk and sputter-coated with a thin layer of gold (samples obtained by layer-by-layer assembly polymerization) or carbon (samples obtained by anodic and chemical oxidative polymerizations) to prevent sample charging problems.

Transmission Electron Microscopy (TEM). TEM images were collected with a Philips TECNAI 10 electron microscope operating at 80 kV. Bright field micrographs were taken with an SIS MegaView II digital camera. Solutions containing PS, PSS, PNCPy/PSS core−shell, and PNCPy hollow spheres (1 mg/1 mL in absolute ethanol) were cast onto a carbon-coated copper grids (300 mesh), the solvent being allowed to evaporate.

FTIR Spectroscopy. Spectra of samples obtained by chemical oxidative polymerization and layer-by-layer assembly polymerizations were recorded on a FTIR 4100 Jasco spectrophotometer with a resolution of 4 cm^{-1} in the transmittance mode. Samples were placed in an attenuated total reflection accessory with a diamond crystal (Specac model MKII Golden Gate Heated Single Reflection Diamond ATR). On the other hand, the spectra of the films generated by electrochemical polymerization were obtained using a Nicolet 6700 FT-IR spectrometer, equipped with a Smart SAGA (Specular Aperture Grazing Angle) accessory with an incidence angle of 80°, gold mirror for background calibration, and Omnic software. The spectrum was taken using a resolution of 4 cm^{-1} in the transmittance mode.

UV−Vis Spectroscopy. Spectra of PNCPy electrochemically generated were obtained using a Shimadzu UV−vis−NIR UV3600 spectrophotometer and with an integrating sphere accessory. All spectra were collected in reflectance mode and converted to absorbance.

RESULTS AND DISCUSSION

PNCPy films obtained by anodic polymerization using $LiClO_4$ as supporting electrolyte and a polymerization time θ = 20 s show a compact, irregular, and lumpy morphology with elliptical protuberances of nanometric dimensions homogeneously distributed in the surface (Figure 1a). Such

dx.doi.org/10.1021/jp3008688 | J. Phys. Chem. B 2012, 116, 5064−5070

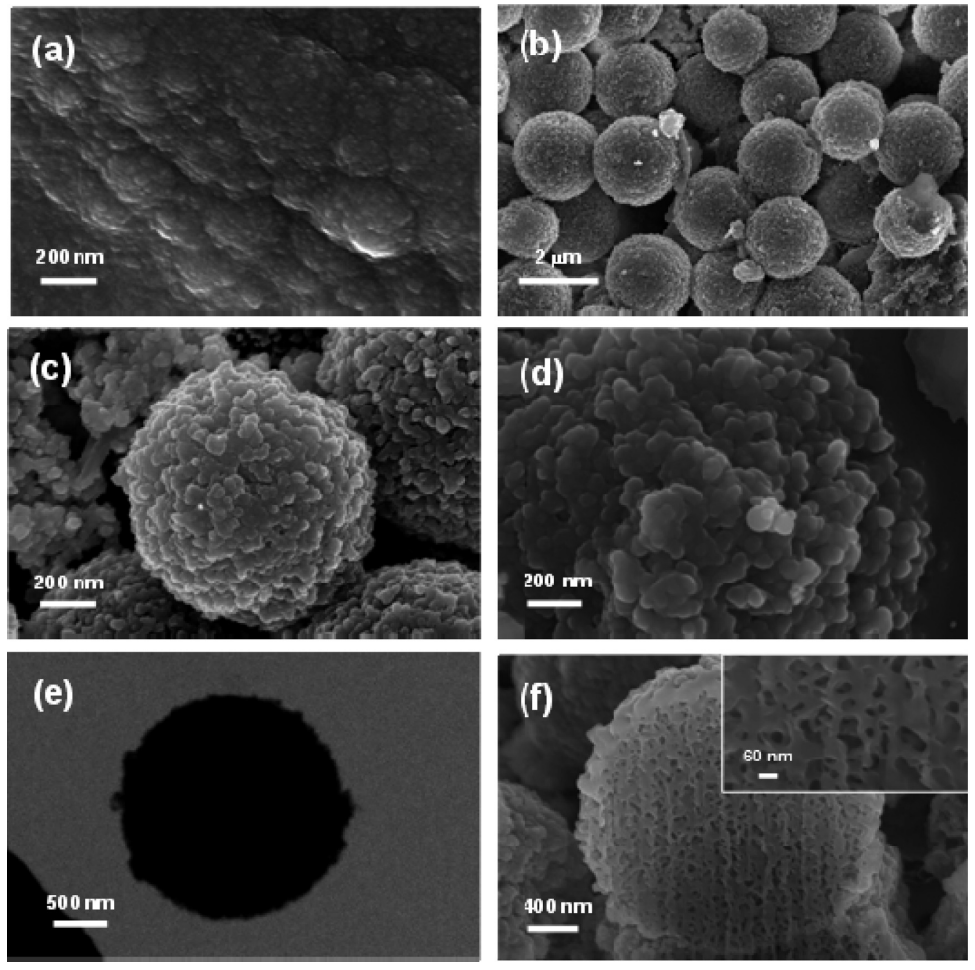

Figure 1. (a) SEM micrograph of the surface of a film prepared by anodic polymerization. (b) Low- and (c) high-resolution SEM images of microspheres obtained using oxidative polymerization in emulsion medium, the pseudospherical nanoaggregates coating the microspheres being displayed in (d). (e) TEM micrographs of an isolated microsphere. (f) SEM image of the FIB-section of a microsphere (inset: high-resolution micrograph showing the remarkable porosity).

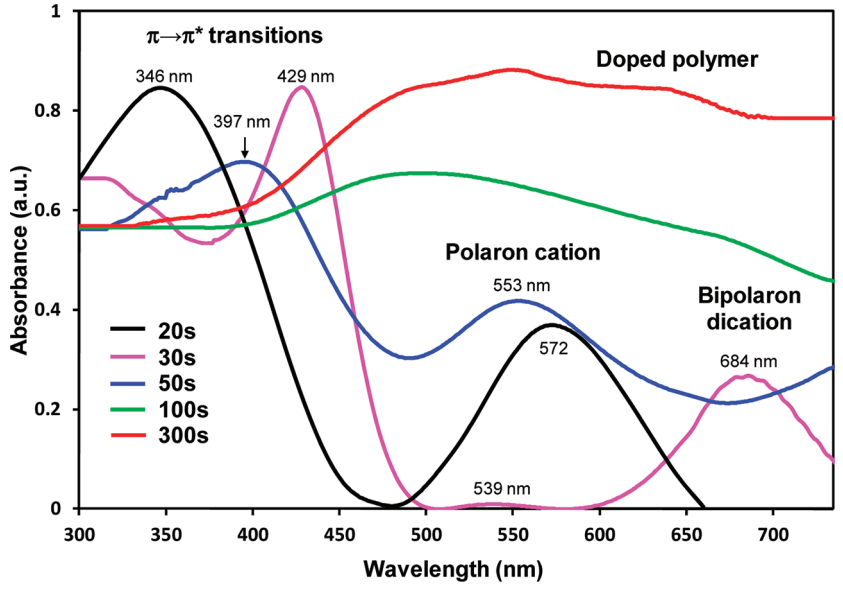

Figure 2. UV−vis spectra of PNCPy obtained using 20, 30, 50, 100, and 300 s of polymerization time and by chronoamperometry. Numbers depicted on the graph are referred to the maximum wavelength obtained for each transition band.

dx.doi.org/10.1021/jp3008688 | J. Phys. Chem. B 2012, 116, 5064−5070

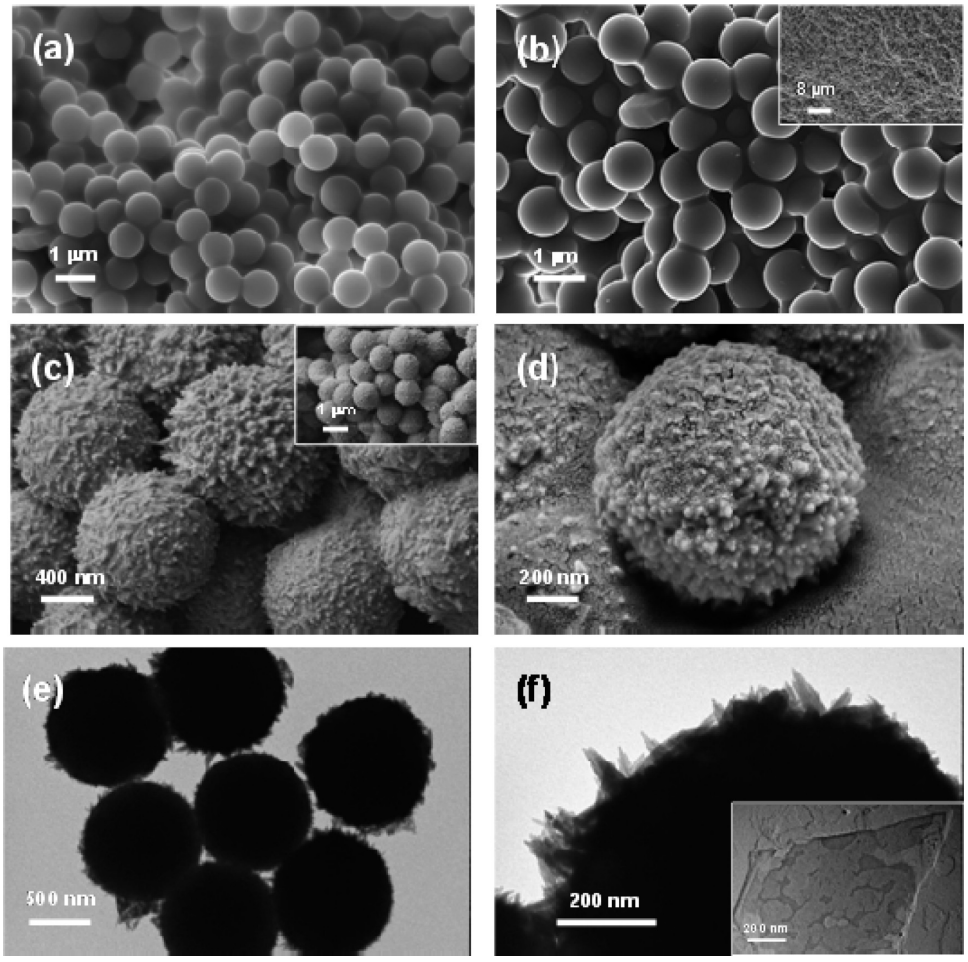

Figure 3. (a,b) SEM micrograph of PS microparticles before and after sulfonation reaction, respectively. (c,d) SEM and (e,f) TEM micrographs of PNCPy/PSS core−shell particles (inset: crystalline structure, shadowed with Pt).

protuberances suggest the formation of small and compact clusters of molecular aggregates. The morphology obtained by electropolymerization should be attributed to the combination of two factors: (i) the influence of the substrate on the growing of polymer chains imposing a directional preference; and (ii) PPy derivatives with substituents at the N-position of the pyrrole ring tend to be cross-linked (i.e., consecutive pyrrole rings may form $\alpha-\beta$ and $\beta-\beta$ linkages in addition to the conventional $\alpha-\alpha$ ones),[29,30] providing branched molecules with many irregularities. The thickness of the films produced using θ = 20 s is 119 ± 16 nm.

UV−vis absorption spectra (Figure 2) revealed that the oxidation level of PNCPy generated electrochemically can be precisely controlled through θ. Thus, the polymer is highly oxidized when θ is higher than 100 s, while the oxidation degree level is very low for θ = 20 s. The first absorption band (before 500 nm) corresponds to the $\pi-\pi^*$ transition of aromatic rings, the maximum absorption being 2.89−3.5 eV. The second absorption band has been assigned to the formation of the polaron cation (~550 nm, 2.1−2.3 eV), which is related to the first stages of the oxidation process, while dications or bipolaronic states (highest oxidation level) show a characteristic absorption at 684 nm (1.81 eV).[31] The UV−vis spectrum of PNCPy generated using θ = 300 s shows a weak absorption at around 350 nm (3.6 eV) and strong absorption in the range of 500−900 nm, the latter being also displayed by the polymer obtained using θ = 100 s. This broad free-carrier-tail band is characteristic of CPs with a high degree of doping. As it can be seen, this situation is completely different from that found for samples produced with lower θ values.

Chemical oxidative polymerization in emulsion medium yielded a powder that corresponds to an aggregation of very well-defined microspheres (Figure 1b and c). The diameters of such microparticles, which were measured directly from the SEM images, ranged from 1.59 to 3.57 μm. The number-average and the volume-average diameters were calculated as $\overline{D}_n = \sum_i N_i D_i / \sum_i N_i$ and $\overline{D}_v = \sum_i N_i (D_i)^4 / \sum_i N_i (D_i)^3$, respectively, where D_i represents the diameters of individual particles and N_i refers to the number of particles corresponding to the diameters. Results indicate that PNCPy microspheres produced using this procedure follow a narrow diameter distribution, with $\overline{D}_n$ = 2.10 μm, $\overline{D}_v$ = 2.36 μm, and $\overline{D}_v/\overline{D}_n$ = 1.12, which is expected to be particularly useful for their possible technological applications. High-resolution micrographs (Figure 1d) obtained by SEM reveal that the surface is coated by compact aggregations of pseudospherical nanoparticles with small and relatively uniform sizes (i.e., $\overline{D}_n$ = 52 nm, $\overline{D}_v$ = 58 nm, and $\overline{D}_v/\overline{D}_n$ = 1.11). Local elemental analyses using EDS revealed the organic nature of such superficial aggregates (i.e., oligomer or polymer chains with a very low amount of iron chloride as dopant), allowing us to discard the deposition of crystalline inorganic iron salts on the surface of the microspheres. TEM micrographs showed that microspheres generated by oxidative

dx.doi.org/10.1021/jp3008688 | J. Phys. Chem. B 2012, 116, 5064−5070

polymerization are solid particles with irregular surfaces (Figure 1e).

The internal structure of the microspheres was investigated after cutting them with focused ion beam (FIB) microscopy and subsequent examination of the section by SEM. Micrographs proved the absence of hollow regions in the core of the microspheres (Figure 1f), which is consistent with the filled structure displayed in the TEM image (Figure 1e). Moreover, high-resolution micrographs reveal a very remarkable porosity that is homogeneously distributed (Figure 1f). The formation of this particular morphology has been attributed to the coexistence of two independent driving forces. First, the formation of spherical microparticles is due to the immiscibility of the NCPy monomer and the mixture of water and ethanol used as emulsion medium. Thus, the micromicelles resulting from such immiscibility define the spherical shape of the polymer microparticles. Second, as mentioned above, PPy derivates substituted at the N-position of the pyrrole ring, including PNCPy,[29,30] tend to form cross-linked structures, giving place to the formation of branched molecules. In electrochemical processes, which are characterized by a directional growing preference (i.e., polymer chains grow perpendicularly to the substrate), cross-linking favors the formation of compact structures. However, the opposite effect is produced when polymer chains grow without any directional preference, as occurs in chemical oxidative polymerization processes. In these cases, cross-linking induces the formation of porous microstructures.

The structural organization displayed in Figure 1b–f suggests that the PNCPy polymerized chemically in emulsion medium may be considered as a potential candidate for technological applications related to molecular transport processes (i.e., loading or encapsulation of molecules and their subsequent releasing through an electric potential). Thus, microspheres for loading and subsequent controlled delivery of therapeutic drugs are frequently prepared using biodegradable polyesters,[32−35] while PPy porous films are used for similar purposes.[36−38] The porous PNCPy microspheres described in this work could be considered as an electric field-stimulus responsive microparticle system for programmed drug loading/delivery. This potential application should be considered complementary to the use of the compact PNCPy films produced by electropolymerization as highly sensitive and effective detectors of dopamine.[24]

Homogeneous solid spherical PS microparticles with an average diameter of 1.0 ± 0.3 μm were prepared using a previously reported procedure (Figure 3a).[28] PSS core/shell particles were obtained through a sulfonation reaction with concentrated sulphuric acid (Figure 3b). It should be noted that surface-sulfonation produces a significant enhancement of the microparticles polarity, the behavior as surfactant of PSS core/shell particles in LbL assembly polymerization processes being reported to be better than that of PS microspheres.[39,40]

PSS microspheres were coated with PNCPy using the LbL assembly technique. More specifically, an ethanol solution of the NCPy monomer was added to the PSS aqueous suspension and, subsequently, stirred for the monomer adsorption on PSS surface. PNCPy then was obtained by chemical polymerization adding $FeCl_3$ as oxidant to the monomer/PSS mixture. This polymerization process was repeated three times to get the desired PNCPy shell thickness and mechanical integrity. The complete synthetic procedure is displayed in Figure 4. The resulting PNCPy/PSS core–shell particles (Figure 3c and d) show very sharp and thin structures on the surface, which are

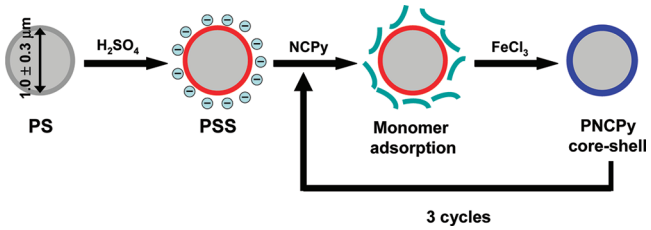

Figure 4. Scheme showing the synthesis of PNCPy core shell microspheres.

completely different from the compact nanoaggregates observed in the microspheres produced by chemical polymerization in emulsion medium (Figure 1c and d). This feature, which was corroborated by TEM (Figure 3e and f), has been attributed to a crystalline organization of oligomers at the surface of the microspheres. Thus, electron micrographs evidenced the presence of crystalline phases with morphology similar to "losango" forms (Figure 3f, inset).

The average thickness of the PNCPy/PSS shell is 54 ± 5 nm after three polymerization cycles, which was taken by SEM from the FIB section (Figure 5a). PNCPy hollow particles were

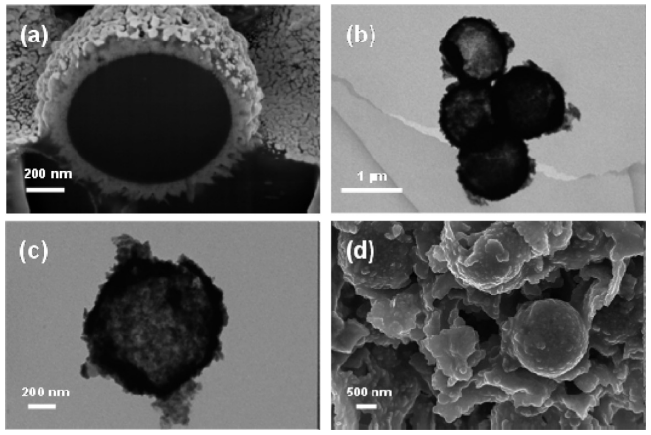

Figure 5. (a) SEM micrograph of the transversal section of a PNCPy/PSS core–shell particle. (b,c) TEM images of free-standing hollow PNCPy microspheres. (d) SEM micrograph of the damage produced by the removal of the PSS template in PNCPy/PSS core–shell microspheres.

obtained after PSS extraction with tetrahydrofuran.[8] TEM images evidenced that removal of PSS was carried out without producing major alterations in the spherical shape of the PNCPy shells (Figure 5b and c), even though some imperfections or defects are detected at the surface of such free-standing hollow microparticles. However, SEM images clearly show serious damages in the integrity of a significant amount of PNCPy microspheres (Figure 5d). Thus, the mechanical properties of PNCPy nanolayers are not good enough to guarantee the integrity of the microspheres once the PSS core–shell particles have been eliminated. Unfortunately, experiments devoted to increase the sell thickness of the PNCPy nanolayer deposition, which was achieved by enlarging the number of polymerization cycles to 4 and 5, did not improve this result. This feature suggests that PNCPy microspheres prepared by the LbL technique are formed by small oligomers, which is consistent with the electron micrograph displayed in Figure 3f. This is a drawback with respect to hollow microspheres produced using other CPs, like

dx.doi.org/10.1021/jp3008688 | J. Phys. Chem. B 2012, 116, 5064–5070

for example PNMPy,[41] even though the technological interest of the latter is smaller than that of PNCPy (i.e., PNMPy shows both lower sensitivity and worse response toward dopamine than does PNCPy).[24]

Despite such limitation in the mechanical properties, we would like to emphasize that polymerization of PNCPy using the LbL technique allows one to obtain spherical particles coated with a shell of CP in which both the size of the particle and the thickness of the shell are precisely controlled. Specifically, the diameter of the particles is defined by the PS templates, while the thickness of the shell is determined by the number of polymerization cycles. Accordingly, nanostructured PNCPy/PSS core−shell particles obtained by LbL may be used for technological applications based on achieve a good dispersion of the CP in a matrix. For example, CPs, including PPy derivatives, have been successfully used as anticorrosive additives in the formulation of organic coatings (i.e., essentially epoxy and alkyd paints),[42−48] imparting corrosion protection to metal substrates when they are well dispersed in the resin. Furthermore, in very recent studies, micro- and nanoparticles of polyaniline, a well-known CP, were used to promote the corrosion protection imparted by epoxy paints.[49] Future studies investigating the potential applications proposed for PNCPy microspheres may allow one not only to expand but also to complement the range of applications covered by this CP. Thus, such applications would depend on the morphology that in turn is controlled through the polymerization procedure.

Samples produced by the three polymerization methods were examined by FTIR spectroscopy. The FTIR spectra allowed us to confirm that th e−C≡N moiety was retained in the polymer structure after polymerization (Figure 6, stretching band at

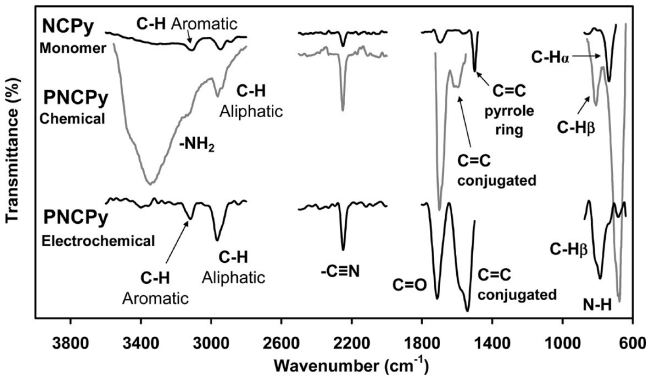

Figure 6. FTIR spectra of PNCPy synthesized by chemical and electrochemical polymerization methods as compared to the monomer (NCPy) absorption bands.

2251 cm^{-1}). However, the oxidation to $-CH_2NH_2$ of a small percentage of nitrile groups was observed in samples prepared using $FeCl_3$ as oxidant agent. Thus, the intensity of nitrile peak decreased while the stretching vibrations of amino group appeared at 3119 and 3200−3500 cm^{-1} (free and hydrogen-bonding associated, respectively), and at 674 cm^{-1} (NH_2 bending). Although the NH_2 group was not observed in electrochemical samples, in which $LiClO_4$ was used as oxidant (strong stretching vibration at 1110 cm^{-1}), the appearance of an intense peak associated with the C═O stretching vibration (1700 cm^{-1}) revealed the overoxidation of the pyrrole ring, as expected.[40,45] Moreover, the absence of C−H^{α} absorption band at 728 cm^{-1} in all of the spectra indicated that the polymerization reactions occurred through the formation of $\alpha-\alpha'$ linkages.

CONCLUSIONS

Our results indicate that the morphology of PNCPy is precisely controlled through the polymerization method. Thus, compact films, solid microspheres with a porous internal structure, and core−shell microspheres with an ultrathin shell have been prepared using anodic, chemical oxidative, and LbL polymerization processes, respectively. Details of all of these microstructures have been obtained using SEM and TEM. Each of these varied morphologies results particularly appropriated for a given technological application.

ASSOCIATED CONTENT

Supporting Information

Particle size distribution of the PNCPy microspheres obtained by chemical oxidative polymerization, and both size distribution and EDX analysis of the nanoaggregates located at the surface of the PNCPy microspheres produced by chemical oxidative polymerization. This material is available free of charge via the Internet at http://pubs.acs.org.

AUTHOR INFORMATION

Corresponding Author

*E-mail: carlos.aleman@upc.edu (C.A.), elaine.armelin@upc.edu (E.A.).

Notes

The authors declare no competing financial interest.

ACKNOWLEDGMENTS

This work has been supported by MICINN-FEDER funds (MAT2009-09138 and MAT2009-11513) and by the Generalitat de Catalunya (2009SGR925, 2009SGR1208, and XRQTC). Support for the research of C.A. was received through the "ICREA Academia".

REFERENCES

(1) Städler, B.; Price, A. D.; Chandrawati, R.; Hosta-Rigau, L.; Zelikin, A. N.; Caruso, F. *Nanoscale* **2009**, *1*, 68−73.
(2) Wang, Y.; Angelatos, A. S.; Caruso, F. *Chem. Mater.* **2008**, *20*, 848−858.
(3) Quinn, J. F.; Johnston, A. P. R.; Such, G. K.; Zelikin, A. N.; Caruso, F. *Chem. Soc. Rev.* **2007**, *36*, 707−718.
(4) Wan, M. *Macromol. Rapid Commun.* **2009**, *30*, 963−975.
(5) Skotheim, T. A.; Reynolds, J. R. In *Handbook of Conducting Polymers*, 3rd ed.; Dyer, A. L., Reynolds, J. R., Eds.; CRC Press: Boca Raton, FL, 2007; Chapter 20.
(6) Invernale, M. A.; Acik, M.; Sotzing, G. A. In *Handbook of Thiophene-Based Materials*; Perepichka, I. F., Perepichka, D. F., Eds.; Wiley-VCH: Chichester, U.K., 2009; Chapter 20.
(7) Poverenov, E.; Li, M.; Bitler, A.; Bendikov, M. *Chem. Mater.* **2010**, *22*, 4019−4025.
(8) Patra, S.; Barai, K.; Munichandraiah, N. *Synth. Met.* **2008**, *158*, 430−435.
(9) Kiefer, R.; Bowmaker, G. A.; Cooney, R. P.; Kilmartin, P. A.; Travas-Sejdic, K. *Electrochim. Acta* **2008**, *53*, 2593−2599.
(10) Aradilla, D.; Estrany, F.; Armelin, E.; Alemán, C. *Thin Solid Films* **2010**, *518*, 4203−4210.
(11) Bund, A.; Neudeck, S. *J. Phys. Chem. B* **2004**, *108*, 17845−17850.
(12) Xia, J.; Masaki, N.; Lira-Cantu, M.; Kim, Y.; Jiang, K.; Yanagida, S. *J. Phys. Chem. C* **2008**, *112*, 11569−11574.

(13) Aradilla, D.; Azambuja, D.; Estrany, F.; Iribarren, J. I.; Ferreira, C. A.; Alemán, C. *Polym. Chem.* **2011**, *2*, 2548−2556.
(14) Parthasarathy, R. V.; Martin, C. R. *J. Appl. Polym. Sci.* **1996**, *62*, 875−886.
(15) Jang, J.; Oh, J. H.; Li, J. *Mater. Chem.* **2004**, *14*, 2872−2880.
(16) Jang, J.; Oh, J. H. *Adv. Mater.* **2003**, *15*, 977−980.
(17) Xia, H. B.; Cheng, D. M.; Xiao, C. Y.; Chan, H. S. O. *J. Mater. Chem.* **2005**, *15*, 4161−4166.
(18) Qu, L.; Shi, G.; Chen, F.; Zhang, J. *Macromolecules* **2003**, *36*, 1063−1067.
(19) Qu, L.; Shi, G. *Chem. Commun.* **2003**, 206−207.
(20) Qu, L.; Shi, G. *J. Polym. Sci., Part A: Polym. Chem.* **2004**, *42*, 3170−3177.
(21) He, X.; Li, C.; Chen, F.; Shi, G. *Adv. Funct. Mater.* **2007**, *17*, 2911−2917.
(22) Li, C.; Bai, H.; Shi, G. *Chem. Soc. Rev.* **2009**, *38*, 2397−2409.
(23) Teixeira-Dias, B.; Alemán, C.; Estrany, F.; Azambuja, D.; Armelin, E. *Electrochim. Acta* **2011**, *56*, 5836−5843.
(24) Fabregat, G.; Córdova-Mateo, E.; Armelin, E.; Bertran, O.; Alemán, C. *J. Phys. Chem. C* **2011**, *115*, 14933−14941.
(25) Aradilla, D.; Estrany, F.; Armelin, E.; Oliver, R.; Iribarren, J. I.; Alemán, C. *Macromol. Chem. Phys.* **2010**, *211*, 1663−1672.
(26) Deng, Z.; Stone, D. C.; Thompson, M. *Can. J. Chem.* **1995**, *73*, 1427−1434.
(27) Deng, Z.; Stone, D. C.; Thompson, M. *Analyst* **1997**, *122*, 1129−1138.
(28) Lascelles, S. F.; Armes, S. P.; Zhdan, P. A.; Greaves, S. J.; Brown, A. M.; Watts, J. F.; Leadley, S. R.; Luk, S. Y. *J. Mater. Chem.* **1997**, *7*, 1349−1355.
(29) Alemán, C.; Casanovas, J.; Torras, J.; Bertran, O.; Armelin, E.; Oliver, R.; Estrany, F. *Polymer* **2008**, *49*, 1066.
(30) Aradilla, D.; Torras, J.; Alemán, C. *J. Phys. Chem. B* **2011**, *115*, 2882.
(31) Okur, S.; Salzner, U. *J. Phys. Chem. A* **2008**, *112*, 11842−11853.
(32) Lee, J.; Oh, Y. J.; Lee, S. K.; Lee, K. Y. *J. Controlled Release* **2010**, *146*, 61−67.
(33) Liu, G.; Miao, X.; Fan, W.; Crawford, R.; Xiao, Y. *J. Biomimetics, Biomater., Tissue Eng.* **2010**, *6*, 1−18.
(34) Freiberg, S.; Zhu, X. X. *Int. J. Pharm.* **2004**, *28*, 1−20.
(35) Crotts, G.; Park, T. G. *J. Controlled Release* **1995**, *35*, 91−105.
(36) Kang, G.; Borgens, B.; Cho, Y. N. *Langmuir* **2011**, *27*, 6179−6184.
(37) Ge, P.; Neofytou, E.; Cahill, T. J.; Beygui, R. E.; Zare, R. N. *ACS Nano* **2012**, *6*, 227−233.
(38) Majumdar, S.; Kargupta, K.; Ganguly, S. *Polym. Eng. Sci.* **2011**, *51*, 2001−2012.
(39) Yang, Y.; Chu, Y.; Yang, F.; Zhang, Y. *Mater. Chem. Phys.* **2005**, *92*, 164−171.
(40) Fu, G.-D.; Li, G. L.; Neoh, K. G.; Kang, E. T. *Prog. Polym. Sci.* **2011**, *36*, 127−167.
(41) Martí, M.; Fabregat, G.; Estrany, F.; Alemán, C.; Armelin, E. *J. Mater. Chem.* **2010**, *20*, 10652−10660.
(42) Hosseini, M. G.; Jafari, M.; Najjar, R. *Surf. Coat. Technol.* **2011**, *206*, 280−286.
(43) Selvaraj, M.; Palraj, S.; Maruthan, K.; Rajagopal, G.; Venkatachari, G. *J. Appl. Polym. Sci.* **2010**, *116*, 1524−1537.
(44) Armelin, E.; Martí, M.; Liesa, F.; Iribarren, J. I.; Alemán, C. *Prog. Org. Coat.* **2010**, *69*, 26−30.
(45) Armelin, E.; Meneguzzi, A.; Ferreira, C. A.; Alemán, C. *Surf. Coat. Technol.* **2009**, *203*, 3763−3769.
(46) Selvaraj, M.; Palraj, S.; Maruthan, K.; Rajagopal, G.; Venkatachari, G. *Synth. Met.* **2008**, *158*, 888−899.
(47) Armelin, E.; Pla, R.; Liesa, F.; Ramis, X.; Iribarren, J. I.; Alemán, C. *Corros. Sci.* **2008**, *50*, 721−728.
(48) Tansug, G.; Tuken, T.; Ozyilmaz, A. T.; Erbil, M.; Yazici, B. *Curr. Appl. Phys.* **2007**, *7*, 440−445.
(49) Jadhav, R. S.; Patil, K. J.; Hundiwale, D. G.; Majulikar, P. P. *Polym. Adv. Technol.* **2011**, *22*, 1620−1627.